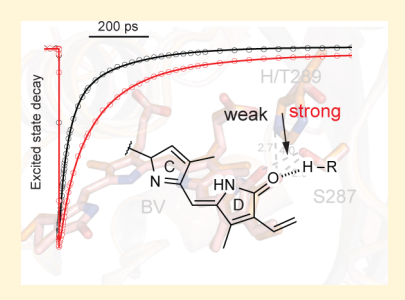


Femto- to Microsecond Photodynamics of an Unusual **Bacteriophytochrome**

Tilo Mathes, Janneke Ravensbergen, Miroslav Kloz, Tobias Gleichmann, Kevin D. Gallagher, Nicole C. Woitowich, *Rachael St. Peter, *Svetlana E. Kovaleva, Emina A. Stojković, * and John T. M. Kennis*,†

Supporting Information

ABSTRACT: A bacteriophytochrome from Stigmatella aurantiaca is an unusual member of the bacteriophytochrome family that is devoid of hydrogen bonding to the carbonyl group of ring D of the biliverdin (BV) chromophore. The photodynamics of BV in SaBphP1 wild type and the single mutant T289H reintroducing hydrogen bonding to ring D show that the strength of this particular weak interaction determines excited-state lifetime, Lumi-R quantum yield, and spectral heterogeneity. In particular, excited-state decay is faster in the absence of hydrogen-bonding to ring D, with excited-state half-lives of 30 and 80 ps for wild type and the T289H mutant, respectively. Concomitantly, the Lumi-R quantum yield is two times higher in wild type as compared with the T289H mutant. Furthermore, the spectral heterogeneity in the wild type is significantly higher



than that in the T289H mutant. By extending the observable time domain to 25 μ s, we observe a new deactivation pathway from the Lumi-R intermediate in the 100 ns time domain that corresponds to a backflip of ring D to the original Pr 15Za isomeric state.

hytochromes are photoreceptor proteins found in plants and bacteria that use covalently bound linear tetrapyrroles as red-light-absorbing chromophores. Their photosensory part is formed by a PAS (Per ARNT Sim), GAF (cGMP phosphodiesterase/adenylyl cyclase/FhlA), and PHY (phytochrome) domain, with the PAS-GAF domains being sufficient to bind the chromophore. The PHY domain is required for the complete photoactivation and downstream signaling. Photoactivation involves isomerization of the C15=C16 double bond from 15Za to 15Ea, $^{2-4}$ which usually results in a photochromic transition between the red-absorbing state Pr to the far red-absorbing state Pfr (Figure 1A). The primary photoproduct, Lumi-R, is formed on the 10 to 100 ps time scale and adopts the 15Ea configuration and evolves within tens to hundreds of microseconds to later intermediates. 5-11 BphP constructs lacking the PHY domain also form a Lumi-R like intermediate but do not form the Pfr state. 12-14

Phytochromes regulate a variety of responses in their respective organisms. Recently, they have been engineered for optogenetic purposes for light-dependent protein localization¹⁵ and light-regulated enzymatic activity. 16,17 In addition, phytochromes recently proved to be potent near-IR markers for deep tissue imaging due to their long emission wavelength. 18-20 Because their fluorescence is usually low, mechanistically inspired improvement of the fluorescence quantum yield is highly desirable.

In canonical phytochromes, the carbonyl of the tetrapyrrole ring D forms a single hydrogen bond (H-bond) to a highly conserved histidine (Figure 1). Toh and coworkers demonstrated that an increased H-bond strength to ring D increases excited-state lifetime and decreases the quantum yield of Lumi-R formation in Rps. palustris RpBphP3 and RpBphP2.8,12 RpBphP3 is an unusual phytochrome with three H-bonds to ring D of BV formed by a serine and a lysine in addition to a highly conserved histidine residue. 13,21 H-bonding to ring D is expected to impair twisting of the C15=C16 double bond in the excited state preceding rupture of ring D H-bonds and final E/Z isomerization of the BV cofactor. In addition, the extent of ring D twisting may activate an excited-state proton transfer (ESPT) channel that deactivates the BV excited state.^{8,12}

To test the effect of a diminished H-bond strength to ring D on photochemical efficiency and excited-state lifetime, we investigated an unusual bacteriophytochrome from the myxobacterium Stigmatella aurantiaca, SaBphP1. This phytochrome contains a threonine at the position of the conserved histidine residue and, according to its recently determined Xray structure of its dark state (PDB ID 4RPW; Woitowich et al, submitted), can be considered devoid of H-bonding to ring D (Figure 1). BphPs from myxobacteria are unique in this property, and it should be noted that some BphPs from other species carrying a mutation of the conserved histidine show

Received: November 13, 2014 Accepted: December 22, 2014 Published: December 22, 2014



[†]Biophysics Group, Department of Physics and Astronomy, Faculty of Sciences, Vrije Universiteit, De Boelelaan 1081, 1081 HV, Amsterdam, The Netherlands

[‡]Department of Biology, Northeastern Illinois University, 5500 North St. Louis Avenue, Chicago, Illinois 60625, United States

The Journal of Physical Chemistry Letters

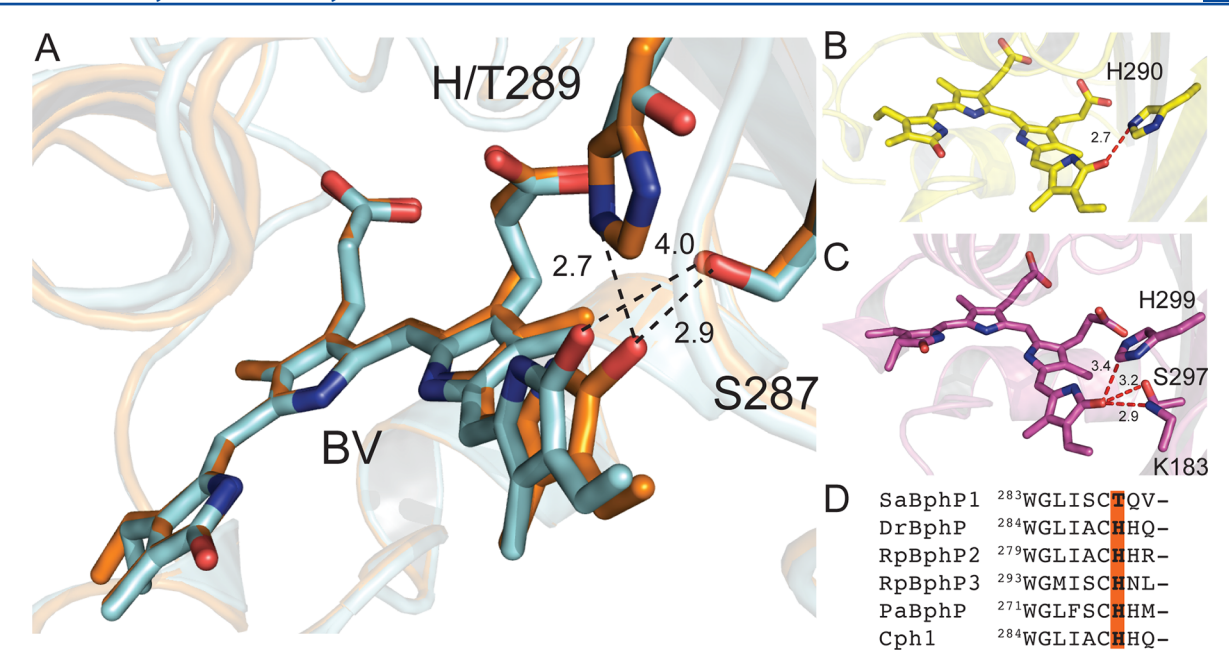


Figure 1. BV binding pocket of SaBphP1 WT (cyan, PDB ID 4RPW) and T289H mutant (orange, PDB ID 4RQ9) observed by X-ray crystallography (A). Hydrogen bonding to ring D in *Deinococcus radiodurans* DrBphP (B, PDB ID 1ZTU) and *Rhodopseudomonas palustris* RpBphP3 (C, PDB ID 2OOL). Sequence alignment of SaBphP1 versus DrBphP, RpBphP3, and other canonical bacteriophytochromes, PaBphP from *Pseudomonas aeruginosa* and Cph1 from *Synechocystis sp.* (C).

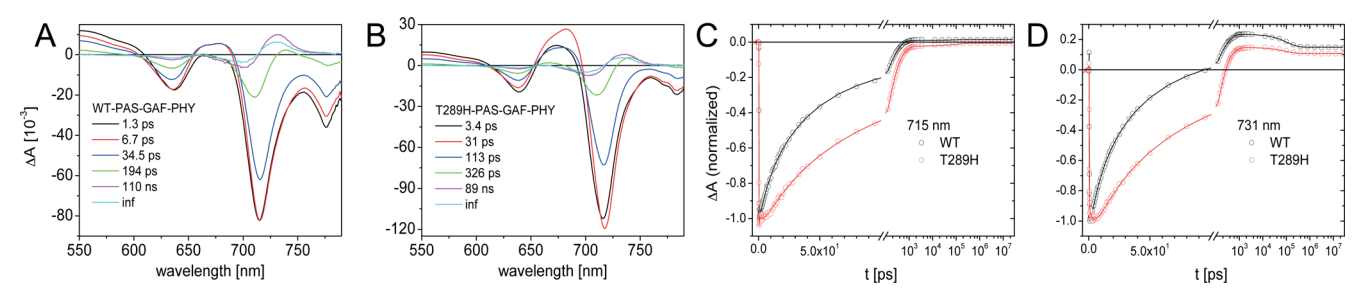


Figure 2. Spectral evolution of SaBphP1 PAS-GAF-PHY wild type (A) and T289H mutant (B) upon excitation at 680 nm, illustrated as evolution-associated difference spectra (EADS) obtained from global analysis. Excited state decay, as visualized by the absorbance change at 715 nm (C), is significantly faster in wild type. The absorption at 731 nm (D) indicates the formation of the Lumi-R intermediate, which appears higher in wild type. The time axis of the plots is linear up to 100 ps and logarithmic hence after.

impaired photoactivity or stability (Woitowich et al., submitted). In contrast, a SaBphP1 mutant containing a single amino acid substitution T289H was successfully constructed, where the threonine was replaced by histidine, and a H-bond to ring D was introduced at this site similar to that of other BphPs (PDB ID 4RQ9; Woitowich et al., submitted). In addition, because of slight rotation of ring D, Ser-287 had come within H-bond distance of ring D, resulting in a double H-bond to ring D. Thus, SaBphP1 provides a rare opportunity to test the effects of H-bonding to ring D on reaction dynamics of phytochromes. Here we report on excited-state lifetimes, Lumi-R quantum yields, and spectral heterogeneity in the wild-type SaBphP1 and the T289H mutant by application of femto-second to microsecond transient absorption spectroscopy.

Absence of Hydrogen Bonding at Ring D Increases Lumi-R Quantum Yield and Speeds up Excited-State Lifetime. In Figure 2 the spectral evolution of SaBphP1 (PAS-GAF-PHY) wild-type and T289H after excitation at 680 nm is displayed as evolution-associated difference spectra (EADS) obtained by global analysis using a model of sequentially interconverting spectra $(1 \rightarrow 2 \rightarrow 3 \rightarrow \cdots)$ with increasing lifetimes. (Raw data are given in Figure S1 in the Supporting Information.) The first

EADS corresponds to the time-zero difference spectrum. This procedure visualizes the evolution of the excited and intermediate states of the system. Six components were necessary for the global fit to adequately represent the data judged by the singular value decomposition of the residual matrix (Figure S2 in the Supporting Information). The first EADS (black) observed in SaBphP1 wild type (Figure 2A) with a 1.3 ps lifetime shows typical excited-state features with ground-state bleaching (GSB) and stimulated emission (SE) at 715 nm and GSB at 625 nm, excited-state absorption (ESA) at below 600 nm and around 675 nm, and SE at ~775 nm. It interconverts into the second EADS (red) without loss in GSB but with an increase of ESA at 675 nm and is considered to reflect a relaxation process, probably structural evolution, in the excited state.8 The second EADS decays into the third EADS with a lifetime of 6.7 ps and represents an overall loss of GSB, ESA, and SE, indicating that the 6.7 ps process corresponds to excited-state decay. The spectral evolution continues with major signal loss in 35 ps into the fourth EADS (green), representing the major component of excited-state decay. The fourth EADS shows GSB and SE but also has a positive signal around 730 nm, which likely corresponds to formation of LumiThe Journal of Physical Chemistry Letters

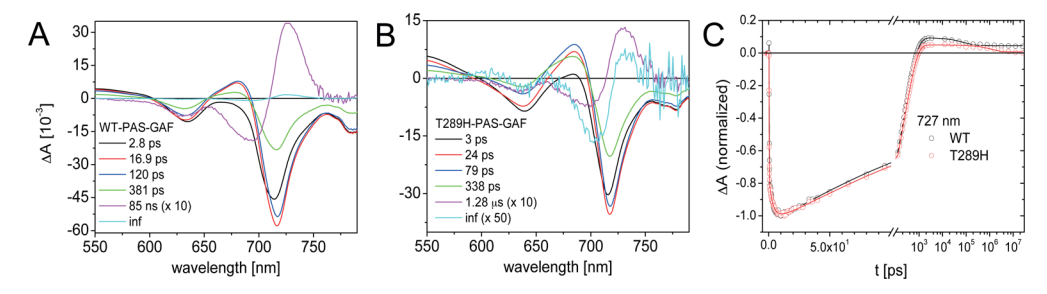


Figure 3. Spectral evolution of SaBphP1 (PAS-GAF). (A) Kinetic traces at 727 nm show the formation of the Lumi-R intermediate. The kinetic behavior of WT and T289H in H_2O are compared in (B). The time axis of the plots is linear up to 100 ps and logarithmic hence after.

R. The fourth EADS further decays in 200 ps into the fifth EADS (magenta), which shows GSB at 700 nm and an induced absorption at 725 nm. This EADS is considered to be representative of the Lumi-R intermediate. The further evolution in 110 ns will be considered in a separate paragraph.

The T289H mutant (Figure 2B) shows a similar spectral evolution but with significantly slower timing on all components, with excited-state decay occurring with time constants of 31, 113, and 326 ps versus the 6.7, 35, and 200 ps time constants of wild type, which is also clearly observed from the kinetic traces at 715 nm (Figure 2C). In terms of excitedstate half-life, wild-type decays in 30 ps versus 80 ps for the T289H mutant. Furthermore, the Lumi-R quantum yield is almost twice as high in wild type as compared with the T289H mutant, estimated from the amplitude of the magenta EADS relative to the initial GSB and by comparison of the normalized kinetic traces at 731 nm (Figure 2D). One apparent difference in the EADS of the mutant is the higher magnitude and spectral shape of ESA at ~675 nm. Similar observations have been made previously on RpBphP2 and RpBphP3, where deletion/ introduction of H-bonds to ring D showed a similar trend.8 Moreover, the magnitude of SE at ~775 nm differs in both proteins and is most likely due to different amount of compensation by ESA.

The PHY domain influences the photochemistry because it indirectly interacts with the BV chromophore via the Hbonding of the conserved PRXSF motif to a conserved aspartate (D208 in SaBphP1).^{22–24} Both PHY domain and aspartate are required to facilitate the photochromic shift, and mutation of either component leads to both an extension of the BV excited-state lifetime and a decrease in Lumi-R quantum yield. 12 Figure 3 shows the EADS and kinetics for the SaBphP1 wild type and T289H PAS-GAF proteins. In accordance with previous results on RpBphP2 and RpBphP3, the excited-state decay is significantly longer than in the corresponding PAS-GAF-PHY domain, with time constants of 80 and 340 ps at about equal amplitude. Interestingly, the excited-state lifetime is basically identical for wild type and T289H, as shown in Figure 3B. The Lumi-R-associated EADS (magenta) is, unlike observed for RpBphP3 and RpBphP2, 12 rather similar to the corresponding PAS-GAF-PHY proteins, with a slight blue shift of the induced absorption but no significant broadening (Figure 3A). Because the relative amplitude to the vibronic groundstate bleach at 640 nm is also very similar, the intermediate is most likely similar to the canonical Lumi-R intermediate in this case, which is formed with much lower quantum yield than in the corresponding PAS-GAF-PHY constructs. In contrast, the corresponding T289H mutant appears to form a species with a deprotonated chromophore similar to the "bleached" Meta-R intermediates (Figure 3B, cyan), as previously observed for

RpBphP3.¹² Accordingly, a different reaction than in WT takes place as spectrally and kinetically illustrated (Figure 3B,C).

We conclude that wild-type SaBphP1 PAS-GAF-PHY, which lacks the H-bond at position 289 to ring D, shows (i) a shorter excited-state lifetime and (ii) an increased Lumi-R quantum yield as compared with T289H mutant, where H-bonds from H289 and S287 to carbonyl group of ring D are formed. For the corresponding PAS-GAF proteins, these phenomena are not or are hardly observed. These observations are in agreement with the trend observed in RpBphP2 and RpBphP3 PAS-GAF-PHY constructs, where increasing the number of H-bonds to ring D from 1 to 3 resulted in longer excited-state lifetime and decrease in Lumi-R quantum yield. Likewise, the differences in this respect between RpBphP2 and RpBphP3 were significantly smaller in their respective PAS-GAF proteins. 12

Absence of Hydrogen Bonding at Ring D Increases Spectral Heterogeneity. The spectral evolution of the studied SaBphP1 samples reveals the presence of significant spectral heterogeneity. This is most clearly visible in the normalized decayassociated difference spectra (DADS, Figure S3 in the Supporting Information). Wild-type SaBphP1 PAS-GAF-PHY has three excited-state decay components of 6.7, 34.5, and 194 ps, and their DADS (Figure S3A in the Supporting Information, red, blue, and green, respectively) differ significantly by GSB maximum and amplitudes of SE and ESA. In T289H PAS-GAF-PHY, the 31 (Figure S3B in the Supporting Information, red) and 113 ps (blue) DADS are nearly identical, while the 326 ps component (green) is blueshifted and differs in extent of SE and ESA, indicating significantly less heterogeneity than in wild type. Likewise, in wild-type SaBphP1 PAS-GAF, the 120 ps (Figure S3C in the Supporting Information, blue) and 381 ps (green) DADS are spectrally shifted and differ in ESA and SE amplitude. In contrast, the T289H PAS-GAF protein shows nearly overlapping DADS of the 79 (Figure S3D in the Supporting Information, blue) and 338 ps (green) components.

The spectral heterogeneity evidenced by the DADS is likely related to distinct ground-state subpopulations that have distinct reaction rates in the excited state.²⁵ Previous studies on bacteriophytochromes in their Pr state by resonance Raman spectroscopy, crystallography, NMR spectroscopy, and transient absorption also documented ground-state heterogeneity consistent with our observations here.^{2,8,14,26–28} The origin of the heterogeneity may, however, differ from case to case and has been attributed to different regions along the tetrapyrrole chain. The missing restraint of ring D in SaBphP1 might be expected to lower the structural heterogeneity of the BV cofactor, which is usually attributed to different H-bonding isoforms of the conserved histidine in classical phytochromes.²⁸

Our observations indicate otherwise: introduction of the conserved histidine in the chromophore binding pocket resulting in the restraint on ring D actually *lowers* the spectral heterogeneity as previously described. Most likely, the conformational freedom due to a missing H-bond to ring D outweighs that provided by multiple H-bonding isoforms, resulting in more distinct ground-state subpopulations in wild type SaBphP1.

Lumi-R Loss on the 100 ns Time Scale: Ring D Back Flip. The spectral evolution of the wild-type SaBphP1 PAS-GAF-PHY protein shows an interesting phenomenon: upon formation of Lumi-R (magenta EADS in Figure 2A), the amplitude of Lumi-R decreases by 30% on a time scale of 100 ns (fifth EADS to sixth EADS, magenta to cyan evolution). The spectrum loses amplitude with a minor blue shift of the induced absorption at 734 nm. A similar process takes place in the corresponding T289H mutant protein (Figure 2B). In principle, two processes could give rise to such a phenomenon: (i) population decay of Lumi-R or (ii) a blue shift of Lumi-R absorption that leads to increased mutual compensation of Pr GSB and Lumi-R absorption, which have opposite signs in the ΔA spectrum. We investigated the second possibility by estimating the absolute Lumi-R spectrum through the addition of the appropriately scaled Pr absorption (Figure S4 in the Supporting Information). We artificially shifted this Lumi-R absorption to the blue to investigate whether this could be the origin of the amplitude decrease. (GSB does not shift upon evolution of transient species.) We found that blue shifting of such a "synthetic" Lumi-R spectrum leads only to a minor amplitude decrease and cannot account for such a drastic loss in amplitude (Figure S4 in the Supporting Information). We conclude that the 100 ns evolution in Lumi-R indicates an overall loss of Lumi-R by 20-30% rather than a shift of the induced absorption band. The final Lumi-R species does not evolve on the time scale of the experiment, which was 25 μ s. To the best of our knowledge, such a Lumi-R amplitude loss on a 100 ns time scale has not been reported before. The observation indicates that photoinduced isomerization of the C15=C16 double bond from 15Za to 15Ea, that is, the formation of Lumi-R, results in a fraction 20-30% of BV isomers, where ring D is not sufficiently stabilized in the 15Ea configuration. Our results indicate that this fraction flips back to 15Za in 100 ns, reforming the original Pr ground state.

In this study, we have mapped out the excited-state properties and reaction dynamics of the unusual bacteriophytochrome SaBphP1 from the myxobacterium Stigmatella aurantiaca, as summarized in Figure 4. In contrast with canonical phytochromes, wild-type SaBphP1 lacks a highly conserved histidine that forms a H-bond with the ring D carbonyl of the tetrapyrrole cofactor. In its single T289H mutant, canonical-like H-bond interactions between H289 and S287 and carbonyl of ring D have been introduced. We demonstrate that the absence of H-bonding to the ring D carbonyl correlates with a shorter excited-state lifetime, with a half-life of 30 ps for wild type and 80 ps for the T289H mutant. In addition, the Lumi-R quantum yield in the absence of Hbonding to the ring D carbonyl is twice as high as compared with that in T289H mutant. We also show that absence of hydrogen-bonding results in an increased ground-state molecular heterogeneity of the chromophore binding pocket in SaBphP1. Furthermore, we report for the first time a decay channel of the Lumi-R intermediate that most likely

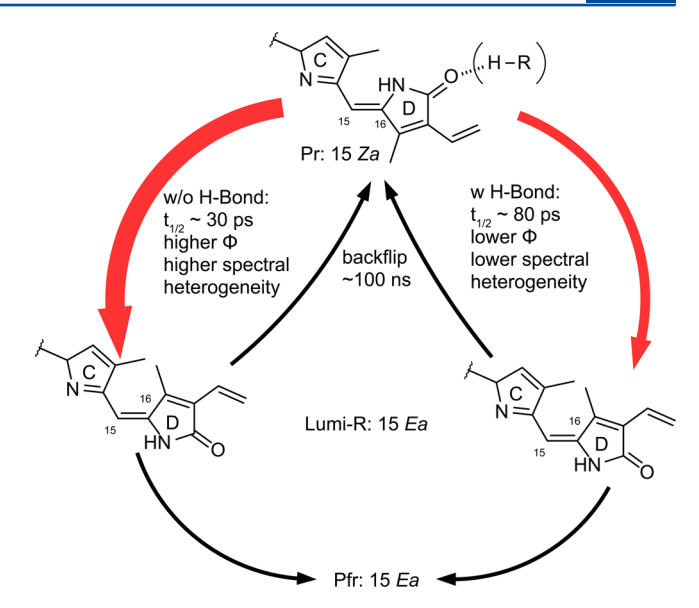


Figure 4. Scheme summarizing reaction dynamics in wild type SaBphP1 and the T289H mutant. See the text for details.

corresponds to a back flip of ring D and reformation of the Pr state of 20–30% of the initially formed Lumi-R.

EXPERIMENTAL METHODS

Proteins were expressed, purified, and treated as previously described. For ultrafast spectroscopy, the proteins were applied to a Lissajous scanner cell at an $\mathrm{OD_{680nm}}\approx0.8$ with 750 nm background illumination. Ultrafast spectroscopy was carried out using a setup previously described. Excitation energy at 680 nm was adjusted to 75 nJ per pulse, and the spot size was $\sim\!0.1~\mathrm{mm^2}$. Time-resolved data were treated for prezero signals as previously described and globally analyzed using the glotaran software package. The proteins were specified as a previously described and globally analyzed using the glotaran software package.

ASSOCIATED CONTENT

S Supporting Information

Experimental details and further spectroscopic data. This material is available free of charge via the Internet at http://pubs.acs.org.

AUTHOR INFORMATION

Corresponding Author

*E-mail: j.t.m.kennis@vu.nl.

Present Address

§T.G.: Laboratory for MEMS Applications, Department of Microsystems Engineering - IMTEK, University of Freiburg, Freiburg, Germany.

Notes

The authors declare no competing financial interest.

ACKNOWLEDGMENTS

T.M., M.K, T.G, and J.T.M.K. were supported by the NWO-Chemical Sciences Section (NWO-CW) through a VICI, Echo, and Middelgroot investment grant to J.T.M.K. M.K. was supported by NWO-CW through a VENI grant. J.R. was supported by the BioSolar Cells Programme of The Netherlands Ministry of Economic Affairs, Agriculture and Innovation. K.D.G. and E.A.S. were supported by NSF MCB 1413360 grant to E.A.S.

REFERENCES

- (1) Rockwell, N. C.; Su, Y. S.; Lagarias, J. C. Phytochrome Structure and Signaling Mechanisms. *Annu. Rev. Plant Biol.* **2006**, *57*, 837–858.
- (2) Yang, X.; Kuk, J.; Moffat, K. Crystal Structure of Pseudomonas aeruginosa Bacteriophytochrome: Photoconversion and Signal Transduction. *Proc. Natl. Acad. Sci. U.S.A.* **2008**, *105*, 14715–14720.
- (3) Rohmer, T.; Lang, C.; Hughes, J.; Essen, L. O.; Gartner, W.; Matysik, J. Light-Induced Chromophore Activity and Signal Transduction in Phytochromes Observed by C-13 and N-15 Magic-Angle Spinning NMR. *Proc. Natl. Acad. Sci. U.S.A.* **2008**, *105*, 15229–15234.
- (4) Mroginski, M. A.; Murgida, D. H.; Hildebrandt, P. The Chromophore Structural Changes during the Photocycle of Phytochrome: A Combined Resonance Raman and Quantum Chemical Approach. *Acc. Chem. Res.* **2007**, *40*, 258–266.
- (5) Andel, F.; Hasson, K. C.; Gai, F.; Anfinrud, P. A.; Mathies, R. A. Femtosecond Time-Resolved Spectroscopy of the Primary Photochemistry of Phytochrome. *Biospectroscopy* **1997**, *3*, 421–433.
- (6) Heyne, K.; Herbst, J.; Stehlik, D.; Esteban, B.; Lamparter, T.; Hughes, J.; Diller, R. Ultrafast Dynamics of Phytochrome from the Cyanobacterium Synechocystis, Reconstituted with Phycocyanobilin and Phycoerythrobilin. *Biophys. J.* **2002**, *82*, 1004–1016.
- (7) van Thor, J. J.; Ronayne, K. L.; Towrie, M. Formation of the Early Photoproduct Lumi-R of Cyanobacterial Phytochrome Cph1 Observed by Ultrafast Mid-Infrared Spectroscopy. *J. Am. Chem. Soc.* **2007**, *129*, 126–132.
- (8) Toh, K. C.; Stojković, E. A.; van Stokkum, I. H. M.; Moffat, K.; Kennis, J. T. M. Proton-Transfer and Hydrogen-Bond Interactions Determine Fluorescence Quantum Yield and Photochemical Efficiency of Bacteriophytochrome. *Proc. Natl. Acad. Sci. U.S.A.* **2010**, *107*, 9170–9175.
- (9) Muller, M. G.; Lindner, I.; Martin, I.; Gartner, W.; Holzwarth, A. R. Femtosecond Kinetics of Photoconversion of the Higher Plant Photoreceptor Phytochrome Carrying Native and Modified Chromophores. *Biophys. J.* **2008**, *94*, 4370–4382.
- (10) Borucki, B.; von Stetten, D.; Seibeck, S.; Lamparter, T.; Michael, N.; Mroginski, M. A.; Otto, H.; Murgida, D. H.; Heyn, M. P.; Hildebrandt, P. Light-Induced Proton Release of Phytochrome Is Coupled to the Transient Deprotonation of the Tetrapyrrole Chromophore. J. Biol. Chem. 2005, 280, 34358–34364.
- (11) von Stetten, D.; Seibeck, S.; Michael, N.; Scheerer, P.; Mroginski, M. A.; Murgida, D. H.; Krauss, N.; Heyn, M. P.; Hildebrandt, P.; Borucki, B.; et al. Highly Conserved Residues Asp-197 and His-250 in Agp1 Phytochrome Control the Proton Affinity of the Chromophore and Pfr Formation. *J. Biol. Chem.* **2007**, 282, 2116—2123.
- (12) Toh, K. C.; Stojkovic, E. A.; van Stokkum, I. H.; Moffat, K.; Kennis, J. T. Fluorescence Quantum Yield and Photochemistry of Bacteriophytochrome Constructs. *Phys. Chem. Chem. Phys.* **2011**, *13*, 11985–11997.
- (13) Yang, X.; Stojkovic, E. A.; Kuk, J.; Moffatt, K. Crystal Structure of the Chromophore Binding Domain of an Unusual Bacteriophytochrome, RpBphP3, Reveals Residues That Modulate Photoconversion. *Proc. Natl. Acad. Sci. U.S.A.* **2007**, *104*, 12571–12576.
- (14) Wagner, J. R.; Zhang, J. R.; von Stetten, D.; Guenther, M.; Murgida, D. H.; Mroginski, M. A.; Walker, J. M.; Forest, K. T.; Hildebrandt, P.; Vierstra, R. D. Mutational Analysis of Deinococcus radiodurans Bacteriophytochrome Reveals Key Amino Acids Necessary for the Photochromicity and Proton Exchange Cycle of Phytochromes. J. Biol. Chem. 2008, 283, 12212–12226.
- (15) Levskaya, A.; Weiner, O. D.; Lim, W. A.; Voigt, C. A. Spatiotemporal Control of Cell Signalling Using a Light-Switchable Protein Interaction. *Nature* **2009**, *461*, 997–1001.
- (16) Gasser, C.; Taiber, S.; Yeh, C.-M.; Wittig, C. H.; Hegemann, P.; Ryu, S.; Wunder, F.; Moeglich, A. Engineering of a Red-Light-Activated Human cAMP/cGMP-Specific Phosphodiesterase. *Proc. Natl. Acad. Sci. U.S.A.* **2014**, *111*, 8803–8808.
- (17) Ryu, M.-H.; Kang, I.-H.; Nelson, M. D.; Jensen, T. M.; Lyuksyutova, A. I.; Siltberg-Liberles, J.; Raizen, D. M.; Gomelsky, M.

- Engineering Adenylate Cyclases Regulated by near-Infrared Window Light. *Proc. Natl. Acad. Sci. U.S.A.* **2014**, *111*, 10167–10172.
- (18) Shu, X.; Royant, A.; Lin, M. Z.; Aguilera, T. A.; Lev-Ram, V.; Steinbach, P. A.; Tsien, R. Y. Mammalian Expression of Infrared Fluorescent Proteins Engineered from a Bacterial Phytochrome. *Science* **2009**, 324, 804–807.
- (19) Filonov, G. S.; Piatkevich, K. D.; Ting, L.-M.; Zhang, J.; Kim, K.; Verkhusha, V. V. Bright and Stable near-Infrared Fluorescent Protein for in Vivo Imaging. *Nat. Biotechnol.* **2011**, *29*, 757–761.
- (20) Shcherbakova, D. M.; Verkhusha, V. V. Near-Infrared Fluorescent Proteins for Multicolor in Vivo Imaging. *Nat. Methods* **2013**, *10*, 751–754.
- (21) Toh, K. C.; Stojkovic, E. A.; Rupenyan, A. B.; van Stokkum, I. H. M.; Salumbides, M.; Groot, M. L.; Moffat, K.; Kennis, J. T. M. Primary Reactions of Bacteriophytochrome Observed with Ultrafast Mid-Infrared Spectroscopy. *J. Phys. Chem. A* **2011**, *115*, 3778–3786.
- (22) Essen, L. O.; Mailliet, J.; Hughes, J. The Structure of a Complete Phytochrome Sensory Module in the Pr Ground State. *Proc. Natl. Acad. Sci. U.S.A.* **2008**, *105*, 14709–14714.
- (23) Takala, H.; Bjorling, A.; Berntsson, O.; Lehtivuori, H.; Niebling, S.; Hoernke, M.; Kosheleva, I.; Henning, R.; Menzel, A.; Ihalainen, J. A.; et al. Signal Amplification and Transduction in Phytochrome Photosensors. *Nature* **2014**, *509*, 245–248.
- (24) Stojkovic, E. A.; Toh, K. C.; Alexandre, M. T.; Baclayon, M.; Moffat, K.; Kennis, J. T. FTIR Spectroscopy Revealing Light-Dependent Refolding of the Conserved Tongue Region of Bacteriophytochrome. *J. Phys. Chem. Lett.* **2014**, *5*, 2512–2515.
- (25) Kim, P. W.; Rockwell, N. C.; Martin, S. S.; Lagarias, J. C.; Larsen, D. S. Dynamic inhomogeneity in the Photodynamics of Cyanobacterial Phytochrome Cph1. *Biochemistry* **2014**, *53*, 2818–2826.
- (26) von Stetten, D.; Gunther, M.; Scheerer, P.; Murgida, D. H.; Mroginski, M. A.; Krauss, N.; Lamparter, T.; Zhang, J.; Anstrom, D. M.; Vierstra, R. D.; et al. Chromophore Heterogeneity and Photoconversion in Phytochrome Crystals and Solution Studied by Resonance Raman Spectroscopy. *Angew. Chem., Int. Ed.* **2008**, 47, 4753–4755.
- (27) Yang, Y.; Linke, M.; von Haimberger, T.; Matute, R.; González, L.; Schmieder, P.; Heyne, K. Active and Silent Chromophore Isoforms for Phytochrome Pr Photoisomerization: An Alternative Evolutionary Strategy to Optimize Photoreaction Quantum Yields. *Struct. Dyn.* **2014**, *1*, 014701.
- (28) Song, C.; Psakis, G.; Lang, C.; Mailliet, J.; Gärtner, W.; Hughes, J.; Matysik, J. Two Ground State Isoforms and a Chromophore D-Ring Photoflip Triggering Extensive Intramolecular Changes in a Canonical Phytochrome. *Proc. Natl. Acad. Sci. U. S. A.* **2011**, *108*, 3842–3847.
- (29) Berera, R.; van Grondelle, R.; Kennis, J. T. M. Ultrafast Transient Absorption Spectroscopy: Principles and Application to Photosynthetic Systems. *Photosynthesis Research* **2009**, *101*, 105–118.
- (30) Ravensbergen, J.; Abdi, F. F.; van Santen, J. H.; Frese, R. N.; Dam, B.; van de Krol, R.; Kennis, J. T. M. Unraveling the Carrier Dynamics of BiVO4: A Femtosecond to Microsecond Transient Absorption Study. *J. Phys. Chem. C* **2014**, *118*, 27793–27800.
- (31) Mathes, T.; van Stokkum, I. H. M.; Stierl, M.; Kennis, J. T. M. Redox Modulation of Flavin and Tyrosine Determines Photoinduced Proton-coupled Electron Transfer and Photoactivation of BLUF Photoreceptors. *J. Biol. Chem.* **2012**, 287, 31725–31738.
- (32) Snellenburg, J. J.; Laptenok, S. P.; Seger, R.; Mullen, K. M.; van Stokkum, I. H. M. Glotaran: a Java-based Graphical User Interface for the R-package TIMP. *J. Stat. Software* **2012**, *49*, 1–22.